Annual Meeting SVGO/ASCO and SBMS 2025

12. June 2025, Inselspital Bern

8:40	Registration
9:00	Welcome from SVGO and SBMS presidents
9:10 – 9:50	**Basic lecture** Cell-metabolic mechanisms leading to iron-induced bone loss *M. Rauner*
9.50	**Short communications** (9' + 3' Q&A) Chair: Serge Ferrari 9:50 Serum Proteomics unveils novel pathways of altered bone metabolism in metabolic syndrome and type 2 diabetes *M. Gerbaix et al.* 10:02 A novel fragility hip fracture risk calculator based on a mechanistic and stochastic modelling approach *C. Wapp et al.* 10:14 Machine learning for the prediction of fragility fractures by bone and body composition parameters: findings from the OsteoLaus 10 years populational cohort *C. Vendrami et al.* 10:26 Prevalences and overlap of major osteoporotic fractures, sarcopenia and frailty in elderly patients with low-impact trauma *R. Plessmann et al.* 10:38 Hormone replacement therapy and the risk of knee and hip replacement: Insights from the OsteoLaus cohort study *J. Geurts et al.*
10.50 – 11:10	Coffee break
11.10	**Clinical lecture** Connect between Fracture prevention - ICOPE and Geroscience *H. Bischoff-Ferrari*
11:35	**Symposium 1: Osteoporosis Management** Chair: Heike Bischoff-Ferrari 11:35 Nutritional Benefits for Bone Health *A. Zittermann* 12:15 Exercise for Osteoporosis Prevention and Treatment *M. Kistler-Fischbacher* 12:30 2025 SVGO osteoporosis treatment guidelines *S. Ferrari*
12:45 – 13:40	Lunch break 13:10-13:40 General meeting SGBOND 13:10-13:40 SVGO General Assembly (room mu5)
13:30-17:00	**SBMS parallel program (see below)**
13:40	**Symposium 2: Inflammatory Diseases and Osteoporosis** Chair: Heike Bischoff-Ferrari 13:40 From Inflammation to Fracture: Autoimmune Diseases and Bone Health *J. Everts*
14:10	**Short communications** (9' + 3' Q&A) Co-Chair: Sigrid Jehle-Kunz, Thierry Chevalley 14:10 Diagnostic value of the calcium load test for the diagnosis of normocalcemic hyperparathyroidism *M. Zampogna et al.* 14:22 Real-World Effectiveness of Romosozumab: A Systematic Literature Review *B. Langdahl et al.*

	14:34 Romosozumab and Teriparatide in Daily Practice: A Retrospective Analysis of German Prescriptions Claims Data *C. Hermsen* 14:46 Patients profile and effectiveness of romosozumab in real-life: a prospective multicenter study in Switzerland *S. Ferrari et al.* 14:58 Impact of Denosumab Discontinuation on Bone Health in Women with Early-Stage Breast Cancer: Insights from the Swiss Prolia Study *L. Campisi et al.*
15:10 – 15:40	Coffee break
15:40	**Symposium 3: Rare Bone Diseases** (70 min) Co-Chairs: Elena Gonzalez, Christian Meier 15:40 Fibrous Dysplasia of bone: Current Insights and Future Directions in Care. *M. Legrand* 16:10 Investigating the effect of metabolic diseases on bone fragility through microscale tissue analysis *J. Schwiedrzik* 16:30 Treatments for rare bone genetic disorders: challenges for the social insurance system *L. Bonafé*
16:50	**Awards ceremony** – Best Presentation Award SBMS – President's Award SBMS: best article – Best Clinical Paper Award (SVGO/ASCO)
17:00	End of the meeting

SBMS AFTERNOON PROGRAM (ROOM Mu5)

FORMAT

Presentations: 7 min talk / 3 min discussion (10 minute slots)

SCHEDULE

13.30 – 13.45
WELCOME & SBMS GENERAL ASSEMBLY

13.45 – 14.45
SESSION 1: IMAGING & NEW TECHNOLOGIES
Moderators: Jeroen Geurts & Cyril Thouverey

13.45 – 13.55
Shape Variability of the Medullary Canal of the Human Proximal Femur
Stefan Bracher – *University of Bern*

13.55 – 14.05
Cellular Uptake and Long-Term Retention of Gadolinium in Bone After Macrocyclic GBCA Exposure
Nathalie Peyer & Ilya Jenni – *University of Bern*

14.05 – 14.15
EasyIPL: A High-Level Scripting Interface for SCANCO MicroCT Image Analysis
Vincent Stadelmann – *Schulthess Clinic Zürich*

14.15– 14.25
A Novel Bioreactor System to Investigate the Biomechanical Characteristics of the Supraspinatus Enthesis
Joshua Dan Spreng – *University of Bern*

14.25– 14.35
Multi- vs. Single-Stack HR-pQCT Scans of Distal Skeleton: Impacts on Geometry, Microarchitecture, and Strength
Simone Poncioni – *University of Bern*

14.35– 15.00 **BREAK**

SESSION 2: BONE BIOLOGY & OSTEOARTHRITIS
Moderators: Benjamin Gantenbein & Vincent Stadelmann

15.00 – 15.10
Human Cortical Bone ECM Proteome: The Fingerprint of Bone Quality
Tatiana Kochetkova – *University of Bern*

15.10 – 15.20
What Keeps Cartilage Attached to Bone? New Details at the Osteochondral Interface
Michael Doube – *City University of Hong Kong*

15.20 – 15.30
In-vivo Quantification of Subchondral Bone Remodeling in Osteoarthritic Rat Knees Using the MIA Model
Antoine Reitzel – *EPF Lausanne*

15.30 – 15.40
Effects of Antidiabetic Medications Liraglutide, Canagliflozin and Metformin on Bone Marrow Adipose Tissue in Knee Osteoarthritis: Insights from an *Ex Vivo* Model
Léa Loisay – *Lausanne University Hospital*

15.40 – 15.50
Inhibition of PDGFRβ Signaling In Lepr^{+} Osteoprogenitors by Long-Term Sclerostin-Neutralizing Antibody Treatment Limits Bone Formation through Progenitor Pool Exhaustion
Cyril Thouverey – *University Hospital of Geneva*

15.50 – 16.00
Uncovering Subchondral Bone and Marrow Cell-Specific Networks in OA Through Integrative Correlation Analysis
Jeroen Geurts – *Lausanne University Hospital*

16.00
END OF SBMS 2025 SCIENTIFIC PROGRAMME

16.20 – 16.45
AWARDS CEREMONY (PRESIDENT & BEST PRESENTATION AWARDS)

17.00-17.05
ASSEMBLY AT REGISTRATION DESK – DEPARTURE SUMMER SCHOOL (INTERLAKEN)

With the kind support of

SANDOZ

AgNovos HEALTHCARE

accord
We make it better

AMGEN 20

GEDEON RICHTER

ALEXION
AstraZeneca Rare Disease

spirig HealthCare
STADA GROUP

VIATRIS

LABATEC
– Valuing People. Science. Life –

KYOWA KIRIN

ucb Inspired by patients. Driven by science.

SVGO/ASCO MORNING SESSION: LIST OF ALL SUBMITTED ABSTRACTS

1. **Diagnostic value of the calcium load test for the diagnosis of normocalcemic hyperparathyroidism.** *Marta Zampogna, Marco Demarchi, Fréderic Triponez, François R Herrmann, Andrea Trombetti*

2. **Prevalences and overlap of major osteoporotic fractures, sarcopenia and frailty in elderly patients with low-impact trauma.** *Plessmann Roxana, Merz Nicola, Eggimann Anna Katharina*

3. **Romosozumab And Teriparatide in Daily Practice: A Retrospective Analysis of German Prescriptions Claims Data.** *Christina Hermsen, Amani Elian, Claudio Schiener, Hans Derk Pannen, Luis Möckel*

4. **Real-World Effectiveness of Romosozumab: A Systematic Literature Review.** *Bente Langdahl, Giovanni Adami, Michael McClung, Kosuke Ebina, Joseph Smith, Stephen Colgan, Jennifer Timoshanko*

5. **Patients profile and effectiveness of romosozumab in real-life: a prospective multicenter study in Switzerland**. *Serge Ferrari, Magaly Hars, Bérengère Aubry-Rozier, Olivier Lamy, Elena Gonzalez Rodriguez, Christian Meier, Sigrid Jehle-Kunz*

6. **A novel fragility hip fracture risk calculator based on a mechanistic and stochastic modelling approach.** *Christina Wapp, Yvan Gugler, Paula Cameron, Alice Dudle, Daniela Frauchiger, Maria Papagerogiou, Emmanuel Biver, Serge Ferrari, Kurt Lippuner, Philippe Zysset*

7. **Serum Proteomics unveils novel pathways of altered bone metabolism in metabolic syndrome and type 2 diabetes**. *Gerbaix Maude, Daniel Courteix, Dutheil Frédérique, Ferrari Serge*

8. **Machine learning for the prediction of fragility fractures by bone and body composition parameters: findings from the OsteoLaus 10 years populational cohort.** Colin Vendrami, Guillaume Gatineau, Elena Gonzalez-Rodriguez, Olivier Lamy, Didier Hans, Enisa *Shevroja*

9. **Hormone replacement therapy and the risk of knee and hip replacement: Insights from the OsteoLaus cohort study.** *Jeroen Geurts, Seda Aydogdu, Cinja Koller, Elena Gonzalez-Rodriguez, Didier Hans, Olivier Lamy, Thomas Hügle, Enisa Shevroja*

10. **Impact of Denosumab discontinuation on bone health in women with early-stage breast cancer: insights from the Swiss Prolia study**. *Lorenzo Campisi, Mohamed Faouzi, Thierry Buclin, Elena Gonzalez Rodriguez, Peter Burkhardt, Olivier Lamy*

ASCO 1

Diagnostic value of the calcium load test for the diagnosis of normocalcemic hyperparathyroidism

Marta Zampogna[1,2] Marco Demarchi[3], Fréderic Triponez[3], François R Herrmann[4], Andrea Trombetti[1]

[1] Division of Bone Diseases, Department of Medicine, University Hospital of Geneva, Geneva, Switzerland; [2] Department of clinical and community science, University of Milan, Milan, Italy, [3] Division of Thoracic and Endocrine surgery, Department of Surgery, University Hospital of Geneva, Geneva, Switzerland; [4]Department of Rehabilitation and Geriatrics, Geneva University Hospitals, Geneva, Switzerland.

Background: Normocalcemic primary hyperparathyroidism (nPHPT) is characterized by elevated parathyroid hormone (PTH) levels with persistently normal calcium levels. The calcium load test (CLTest) has been suggested in the literature as a tool to distinguish nPHPT patients from patients with secondary hyperparathyroidism, by assessing PTH suppression after calcium administration. The aim of this study is to evaluate the effectiveness of the calcium load test in diagnosing nPHPT at the University Hospitals of Geneva (HUG).

Methods: Retrospectively, we analyzed patients operated for nPHPT (n=91) at HUG between 2012 and 2025. Among them, 19 had a positive CLTest before surgery (group A), and 72 did not perform a CLTest (group B). The CLTest consisted by administering 1 g of oral calcium, followed by intravenous calcium gluconate at 2 mg/kg. It is considered positive if at least one of the PTH suppression criteria published in the literature is met.

Results: All patients in group A had histological disease confirmation of parathyroid disease, while 5% (4/72) in group B did not (p=0.29). Multiglandular disease was detected in 47% (9/19) of patients in group A and 29% (21/72) in group B (p=0.13). During the 6 months following surgery, 5% (1/19) in group A had persistent elevation of PTH compared with 21% (15/72) in group B (ns).

Conclusions: The CLtest is useful in clinical practice to support the diagnosis of nPHPT, alongside localization studies. In our experience, all patients with a positive CLtest who underwent surgery had histopathological confirmation of parathyroid disease.

ASCO 2

Prevalences and overlap of major osteoporotic fractures, sarcopenia and frailty in elderly patients with low-impact trauma

Plessmann, Roxana[1], Merz, Nicola[1], Eggimann, Anna Katharina[2]

[1] University of Bern, Medical Faculty, Bern, Switzerland, [2] Department of Geriatrics, Inselspital, Bern University Hospital, University of Bern, Bern, Switzerland

Background: We want to present up-to-date prevalences of major osteoporotic fractures (MOF), sarcopenia and frailty and their gender specific differences in elderly patients hospitalised with low-impact trauma.

Hypothesis: We think there is a substantial overlap between MOF, sarcopenia and frailty.

Methods: Data of an observational study in Switzerland were analysed from 112 acutely hospitalised patients, 70 years and older, with low-impact trauma between June 2024 and January 2025. MOF are defined as fractures of hip, vertebral, humerus and/or forearm. Sarcopenia was measured using handgrip strength and point-of-care ultrasound of rectus femoris applying validated cut-offs (EWGSOP2). Frailty was defined as Clinical Frailty Scale >= 5 Points. Prevalences are shown descriptively. Gender specific differences were analysed using chi2 test.

Results: In 112 patients (72.3% women), mean age was 81.0 years (standard deviation 6.9 years). 62 (55.4%) patients showed a MOF, 38 (33.9%) sarcopenia and 41 (36.6%) frailty. An overlap between those showed in 9 (8.0%) patients. There was no significant difference for MOF prevalence in women vs. men (54.3% vs. 58.1%, p=0.7) as well as for frailty (32.1% vs. 48.4%, p=0.1). There was a significant difference in prevalence of sarcopenia in men vs. women (53.3% vs. 28.6%, p=0.02). This difference is explained by a gender specific difference in the hand grip.

Conclusion: The prevalences of MOF, sarcopenia and frailty are substantial with an overlap in 1:12.5 patients. There is a gender specific difference in the prevalence of sarcopenia, especially in hand grip requiring further investigations in the defined cut-offs for hand grip.

ASCO 3

Romosozumab And Teriparatide in Daily Practice: A Retrospective Analysis of German Prescriptions Claims Data

Christina Hermsen,[1] Amani Elian,[2] Claudio Schiener,[2] Hans Derk Pannen,[1] Luis Möckel[1]

[1]UCB, Monheim am Rhein, Germany; [2]Insight Health GmbH, Waldems-Esch, Germany

Presenting on behalf of the authors: Sonja Giger: UCB Pharma, Bulle, Switzerland

Background: Romosozumab and teriparatide are osteoanabolic agents recommended for patients at very high risk of fracture.

Hypothesis: We describe patient characteristics and treatment persistence in romosozumab or teriparatide patients in Germany.

Methods: Retrospective analysis of German prescription claims from the Insight Health database (covering ~64 million statutorily health-insured patients) was conducted. Patients with ≥1 prescription of romosozumab or teriparatide between January 2017-October 2023 were included. 12-months persistence was analysed between March 2020-October 2023, using 90- and 180-day drop-out criteria without censoring patients lost to follow-up at the end of the study period.

Results: Patients with romosozumab (n=2,252) and teriparatide prescriptions (n=4,927) were included.
Romosozumab patients were mostly aged 60-69 (34.6%) and 70-79 years (26.9%); teriparatide patients were mostly aged 80+ (32.0%) and 70-79 years (25.7%). Only 4.0% and 11.9% of romosozumab- and teriparatide-treated patients, respectively, were treatment-naïve. For romosozumab and teriparatide patients, the most frequent prior treatments were alendronate (33.6%/35.0%), denosumab (20.2%/16.0%), and ibandronate (16.1%) for romosozumab, and risedronate (15.1%) for teriparatide.
At 12-months, persistence was 65.5% in romosozumab patients and 52.6% for teriparatide (90-day drop-out criterion). With the 180-day drop-out criterion, persistence was 67.2% and 56.8%, respectively. Romosozumab was most often followed by denosumab (51.0%), zoledronate (17.8%) and alendronate (13.5%). Teriparatide was followed by denosumab (42.6%), alendronate (17.3%) and zoledronate (10.6%).

Conclusions: Patients treated with romosozumab were younger than teriparatide patients and showed numerically higher persistence. Contrary to new DVO guidelines (2023) recommending osteoanabolic treatment first, most patients were not treatment-naïve before starting romosozumab or teriparatide.

Funding: UCB/Amgen.

ASCO 4

Real-World Effectiveness of Romosozumab: A Systematic Literature Review

Bente Langdahl,[1] Giovanni Adami,[2] Michael McClung,[3] Kosuke Ebina,[4] Joseph Smith,[5] Stephen Colgan,[6] Jennifer Timoshanko[7]

[1]Aarhus University Hospital and Aarhus University, Aarhus, Denmark; [2]University of Verona, Verona, Italy; [3]Oregon Osteoporosis Center, Portland, Oregon, USA; [4]Osaka University, Osaka, Japan; [5]Costello Medical, Cambridge, UK; [6]Amgen, Thousand Oaks, California, USA; [7]UCB, Slough, United Kingdom

Presenting on behalf of the authors: Sonja Giger: UCB, Bulle, Switzerland

Background: Romosozumab is a sclerostin inhibitor approved globally for the treatment of people with osteoporosis (OP) at high risk of fracture. Romosozumab increases bone formation and decreases bone resorption.

Hypothesis: We summarise observational, real-world evidence for use of romosozumab.

Methods: An SLR was conducted according to PRISMA guidelines. MEDLINE, Embase and conference proceedings were searched to 2nd December 2024 for observational studies of patients receiving romosozumab reporting effectiveness outcomes.

Results: The SLR identified 613 records; 54 studies across 12 countries were included. Most were retrospective cohort studies (n=33) and 20/54 were comparative. Number of patients for romosozumab (range): 10-16,125; comparators: 21-33,057. Mean patient age: 52.3-84.4 years. Across romosozumab and comparators, mean bone mineral density (BMD; T-score) at baseline ranged from –3.80 to –1.70 (lumbar spine [LS]), –3.10 to –2.20 (total hip [TH]), and –3.70 to –2.20 (femoral neck [FN]).
Mean percentage change in LS BMD at 12 months ranged from 6.80%-15.60% and 1.30%-10.20% for romosozumab- and comparator-treated patients, respectively. Mean percentage change in TH BMD ranged from –0.90%-6.60% (romosozumab) and –0.90%-3.60% (comparators) with similar changes in FN BMD. Romosozumab was associated with significant improvements in BMD at 12 months versus baseline in 15/15 (LS), 11/12 (TH) and 11/14 (FN) studies. BMD gains in treatment-naïve patients were significantly larger compared with previously treated patients, in 6/9 (LS), 4/8 (TH) and 2/6 (FN) studies.

Conclusions: Romosozumab improved BMD and demonstrated larger BMD gains versus comparators at 12 months. Effectiveness was reduced in previously treated patients, highlighting treatment sequencing importance.

Funding: UCB

ASCO 5

Patients profile and effectiveness of romosozumab in real-life: a prospective multicenter study in Switzerland

Serge Ferrari[1], Magaly Hars[1], Bérengère Aubry-Rozier[2], Olivier Lamy[3], Elena Gonzalez Rodriguez[3], Christian Meier[4], Sigrid Jehle-Kunz[5]

[1] Division of Bone Diseases, Geneva University Hospitals and Faculty of Medicine, University of Geneva, Geneva, Switzerland
[2] FMH Rheumatology and Bone Diseases, Lausanne, Switzerland
[3] Interdisciplinary Center of Bone Diseases, Lausanne University Hospital and University of Lausanne, Lausanne, Switzerland
[4] Division of Endocrinology, Diabetology and Metabolism, University Hospital and University of Basel, Basel, Switzerland
[5] Center for Osteoporosis, St. Anna Clinic, Lucerne, Switzerland

Objective: Romosozumab (Romo) is a monoclonal antibody against sclerostin with dual antiresorptive and anabolic effects. This study aimed to determine patients' profile receiving Romo and evaluate effectiveness of one-year treatment in high-risk osteoporosis patients, in routine clinical practice.

Methods: This prospective study was conducted in five osteoporosis centers in Switzerland among patients who initiated 12 months of treatment with Romo (210 mg subcutaneously monthly) since 2021. The primary outcome was bone mineral density (BMD) changes from baseline to 12 months at lumbar spine (LS), total hip (TH), and femoral neck (FN). Data on bone turnover markers (BTM), carboxy terminal telopeptide of collagen type I (CTX) and procollagen type 1 N-terminal propeptide (P1NP) were also collected.

Results: A total of 340 patients (89.7% female) with mean (±SD) age of 70.4 (±10.3) years were enrolled in this study. Among them, 48.8% were treatment-naïve while 22.9% switched from bisphosphonate or denosumab to Romo and 28.2% received osteoporosis treatment in the past. At Romo initiation, 71.2% had experienced multiple major osteoporotic

fracture, 78.5% a recent fracture, and a T-Score ≤ -3.5 was found in half of the patients. In patients who completed the 12-dose course of Romo treatment
(86.9%) the median BMD percentage changes from baseline to 12 months were 12.9% at
LS, 3.0% at TH, and 3.1% at FN. In patients who discontinued Romo before 12 months (median exposure of 5 months; range 1-11), comparable BMD gains to 12 months completers were observed at LS and FN at month 12, but BMD gains at total hip were lower. BMD gains were significantly higher at all sites in treatment-naïve patients compared to the group previously exposed to anti-resorptives.

Conclusion: This real-world data in a population of Swiss patients contributed to the growing body of evidence that Romo treatment for 12 months substantially increased BMD at LS, FN, and TH in patients at high fracture risk. The increase in BMD was attenuated in patients switching from antiresorptive therapy to Romo compared to treatment-naïve patients, and potentially at the hip in those interrupting treatment prematurely.

Acknowledgement: This study was sponsored by UCB Pharma.

ASCO 6

A novel fragility hip fracture risk calculator based on a mechanistic and stochastic modelling approach

Christina Wapp[1], Yvan Gugler[1], Paula Cameron[1], Alice Dudle[1] Daniela Frauchiger[1,2], Maria Papagerogiou[3], Emmanuel Biver[3], Serge Ferrari[3], Kurt Lippuner[2], Philippe Zysset[1]

[1]ARTORG Center for Biomedical Engineering Research, University of Bern, Bern, Switzerland [2]Department of Osteoporosis, Inselspital, Bern University Hospital, University of Bern, Bern, Switzerland
[3]Division of Bone Diseases, Department of Medicine, Geneva University Hospitals and Faculty of Medicine, University of Geneva, Geneva, Switzerland

Fragility fractures of the hip in older adults are a major burden for the individual and society, as they result in increased morbidity, mortality and substantial health care expenditure. Most hip fractures are caused by falls resulting in an impact on the hip, inducing a force that exceeds the femoral bone strength. The risk of fracture depends on the rate of falling and the fall-induced impact force in relation to femoral bone strength. This work presents the framework of a novel personalised fragility hip fracture risk calculator based on a stochastic and mechanistic modelling approach, integrating the stochastic aspects of a fall together with a 1D dynamic mechanical model computing the impact force in the hip to calculate a one-year absolute fracture risk. The required input variables require solely anthropometric and densitometric data and can be refined using QCT images. Thus, the calculator does not depend explicitly but implicitly on epidemiological risk factors such as age, sex or ethnicity. A sensitivity analysis assessing the influence of the model's variables on the fracture risk was conducted, confirming that the fall rate, the trochanteric soft tissue thickness and the bone strength are the dominating factors influencing the risk of fragility fractures of the hip. Furthermore, output variables such as the predicted impact velocity and impact force aligned well with experimental data. Thus, the model is able to reflect observations from empirical data, indicating that it can capture the intrinsic aspects that affect the risk of fragility hip fractures.

ASCO 7

Serum Proteomics unveils novel pathways of altered bone metabolism in metabolic syndrome and type 2 diabetes

Gerbaix Maude [(1)], Daniel Courteix [(2)], Dutheil Frédérique [(2)], Ferrari Serge [(1)]

[1]Division of Bone Diseases, Geneva University Hospitals and Faculty of Medicine, Geneva, Switzerland,2
[2]Université Clermont Auvergne, CHU Clermont-Ferrand, University Hospital of Clermont-Ferrand

Type 2 Diabetes Mellitus (T2D) is associated with low bone turnover and fragility despite normal-to-high bone mineral density (BMD), and often coexists with Metabolic Syndrome (MetS), characterized by central obesity, dyslipidemia, hypertension, and impaired fasting glucose. We previously showed that MetS and T2D progressively reduce bone turnover while increasing BMD, though underlying mechanisms remain unclear. This study employed a proteomic approach to explore regulatory pathways of altered bone metabolism in MetS and T2D.

Serum proteomic profiles were assessed via liquid chromatography-tandem mass spectrometry (LC-MS/MS) in age-matched men and women with MetS (59±5 yrs; n=26), MetS-T2D (60±5 yrs; n=26), and healthy controls (Ctr; 60±5 yrs; n=26). Of 541 proteins analyzed, 56 differed between MetS and Ctr, 75 between MetS-T2D and Ctr, and 26 between MetS-T2D and MetS. Among them, PEDF was upregulated in MetS and MetS-T2D vs Ctr (+6%; +23%; $p<0.05$), correlating positively with HbA1c, spine and hip BMD, and negatively with CTX. IGFBP2 was downregulated (-42%; -54%; $p<0.0001$), correlating negatively with HbA1c and hip BMD, and positively with OCN, P1NP, and CTX. Gene ontology analysis identified pathways in lipid transport, cholesterol metabolism, inflammation, and extracellular matrix (ECM) degradation. LBP was upregulated (+30%; +41%; $p<0.05$), correlating positively with HbA1c and negatively with P1NP. CRP was elevated (+137%; +194%; $p<0.05$), correlating negatively with P1NP and CTX. MMP-9 increased (+78%; +56%; $p<0.05$), inversely associated with OCN, P1NP, and CTX.

These findings reveal novel systemic and bone-derived proteins potentially contributing to diabetic bone fragility through osteoblast dysfunction, lipid handling, inflammation, and ECM remodeling.

ASCO 8

Machine learning for the prediction of fragility fractures by bone and body composition parameters: findings from the OsteoLaus 10 years populational cohort

Colin Vendrami[1,2], Guillaume Gatineau[1], Elena Gonzalez-Rodriguez[1], Olivier Lamy[1,2], Didier Hans[1], Enisa Shevroja[1]

[1]Interdisciplinary Center of Bone Diseases, Rheumatology Unit, Bone and Joint Department, Lausanne University Hospital and University of Lausanne, Switzerland, Lausanne, Switzerland,

[2]Department of Medicine, Internal Medicine, Lausanne University Hospital and University of
Lausanne, Switzerland, Lausanne, Switzerland

Background: Recent reviews highlighted the potential value of machine learning (ML) in improving fragility fracture prediction.

Hypothesis: We aim to analyse the prediction of fragility fractures using regional and total body Dual X-ray Absorptiometry (DXA) assessments using a ML pipeline.

Methods: 1475 Swiss post-menopausal women (mean 63.3±7.1 years, BMI 25.4±4.3kg/m^2) were followed for 10 years (2010-2022). Parameters of bone health (hip and spine DXA: 34 variables) and body composition (total body DXA: 65 variables) were assessed by DXA scans. Vertebral fractures were screened with lateral DXA. Other risk factors (15 variables) and fragility fractures were collected from questionnaires. All datasets were split for training (85%) and testing (15%) with a balanced fragility fractures proportion. 8 ML models were trained with hyperparameters tunning through 5-fold cross-validation to maximize the area under the curve (AUC).

Results: 590 to 957 participants were included in the final complete case analyses, with 115-221 fragility fractures. The combination of all 114 variables in the same dataset achieved the best AUC in both train set (1.00-0.70) and test set (0.79-0.64). Logistic regression demonstrated the best balance in performance metrics: AUC 0.78, specificity 0.82, sensitivity 0.71. ML models tend toward higher sensitivity and lower specificity.

Conclusions: These findings emphasize the combination of DXA-derived bone and body composition parameters for fragility fracture prediction. Logistic regression produced the most promising results. ML models remain at interest for further analysis in combination with image based analysis. Further studies including a comparison with FRAX®, larger sample size and external validation are needed.

ASCO 9

Hormone replacement therapy and the risk of knee and hip replacement: Insights from the OsteoLaus cohort study

Jeroen Geurts[1], Seda Aydogdu[1], Cinja Koller[1], Elena Gonzalez-Rodriguez[2], Didier Hans[2], Olivier Lamy[2], Thomas Hügle[1] , Enisa Shevroja[2]

[1]Rheumatology, CHUV-UNIL [2]Interdisciplinary Centre for Bone Diseases, CHUV-UNIL

Introduction: The relationship between hormone replacement therapy (HRT) and joint replacement risk remains debated due to inconsistent findings.

Hypothesis: Longer duration of hormone replacement therapy (HRT) use is associated with an increased incidence of total knee replacement (TKR) and hip replacement (THR) among postmenopausal women.

Methods: A population-based cohort study was conducted using data from the OsteoLaus study (2010–2022), including 1,026 women with ≥7.5 years of follow-up. Participants with prior joint replacement or hip fracture were excluded (n=87). TKR and THR were identified through DXA imaging. Cox proportional hazard models assessed associations between HRT status (never, past, current), duration, and joint replacement, adjusting for age, BMI, femoral neck BMD, calcium/osteoporotic drug use, comorbidities, ΔBMI, ΔBMD, HRT start age, and follow-up duration.

Results: TKR and THR incidence rates were 7.0 and 6.1 per 1,000 person-years. Participants with TKR or THR were older, had higher BMI (TKR only), and higher femoral neck BMD. No significant differences were found in baseline HRT use between cases and controls. Current HRT use was not associated with incident TKR (HR 1.46, 95% CI 0.92–2.31) or THR (HR 1.34, 95% CI 0.67–2.67). However, longer baseline HRT duration was linked to higher TKR risk (HR 1.06 per year, 95% CI 1.01–1.11), but not THR.

Conclusion: Prolonged HRT use was associated with increased TKR risk, but not THR, suggesting differing underlying mechanisms. Further investigation, particularly in older populations, is warranted.

ASCO 10

Impact of Denosumab Discontinuation on Bone Health in Women with Early-Stage Breast Cancer: Insights from the Swiss Prolia Study

Lorenzo Campisi[1], Mohamed Faouzi[2], Thierry Buclin[3], Elena Gonzalez Rodriguez[1], Peter Burkhardt[3], Olivier Lamy[1]

[1]Interdisciplinary center of Bone Diseases, Lausanne university hospital, Switzerland
[2]University Center for Primary Care and Public Health Biostatistics, Lausanne university hospital, Switzerland
[3]University of Lausanne, Faculty of Biology and Medicine, Lausanne university hospital, Switzerland

Objective(s): To evaluate the effects of denosumab (Dmab) discontinuation (DD) on vertebral fracture (VF) risk in postmenopausal women with early-stage breast cancer (ESBC) undergoing adjuvant aromatase inhibitor therapy; to identify associated risk and protective factors.

Material and Methods: Data derived from the Swiss Prolia Study cohort included 797 postmenopausal women (134 ESBC) treated with Dmab. All received ≥ 2 injections and were followed for ≥30 months post-discontinuation. Key outcomes included VF prevalence, multiple VF (MVF) and total VF count. Bone turnover markers (BTM), bone mineral density (BMD) and fracture occurrence were analyzed across three periods: before, during and after discontinuation. Statistical analyses utilized Cox proportional hazard models and logistic regression.

Results: At baseline, ESBC patients were younger (mean age 62 vs 66 years, p<0.001), had higher baseline BMD (at all sites p<0.001), less VF and non-VF, and were less pretreated with bisphosphonates (BP) (22% vs 53%, p<0.001) than women without BC (WBC). ESBC patients received more Dmab doses (6.7 vs 5.7, P=0.002). After DD, 62.7% of ESBC patients received BP (vs 67.1% in WBC); BMD decreased significantly at all sites, more pronounced in ESBC. 17 ESBC patients (12.7%) had 46 VFs of whom 13 (10%) had MVF (3.2VF/patient). In WBC, 65 (9.8%) had 169 VF, 47 (7.1%) had MVF. Prior VFs and elevated BTMs after DD were strongly associated with the risk of VF after DD. No protective factor was identified. Non-VF were rare, with no cases after DD in ESBC.

Conclusion(s):DD in ESBC patients is associated with a high risk of VF, particularly MVF, despite higher BMD and younger age. Our findings highlight the importance of

cautious decision-making regarding Dmab initiation, particularly in younger
women or with higher BMD. Incorporating BP into the therapeutic regimen before or during the rebound period may reduce fracture risk[1-2], especially in those at low fracture risk.

References:1- Burckhardt P, Faouzi M, Buclin T, Lamy O, The Swiss Denosumab Study Group. Fractures After Denosumab Discontinuation: A Retrospective Study of 797 Cases. J Bone Miner Res 2021;36(9):1717–28.
2 - Jain S. Prevention and Management of Denosumab Discontinuation Rebound Fractures. Endocrinol Metab Clin North Am 2024;53(4):559–83.

Disclosures (if applicable): No conflicts of interest were disclosed.

SBMS AFTERNOON SESSION: LIST OF ALL SUBMITTED ABSTRACTS

1. **Shape Variability of the Medullary Canal of the Human Proximal Femur.** *Stefan Bracher, Benjamin Haas, Elhadi Sariali, Philippe Zysset*

2. **A novel bioreactor system to investigate the biomechanical characteristics of the supra spinatus enthesis.** *Ćorluka Slavko, Spreng Joshua Dan, Gantenbein Benjamin, Schär Michael*

3. **What keeps cartilage attached to bone? New details at the osteochondral interface.** *Khizar Hayat, Aimee Colbath, Michael Doube*

4. **Uncovering Subchondral Bone and Marrow Cell-Specific Networks in Osteoarthritis through Integrative Correlation Analysis.** *Jeroen Geurts, Léa Loisay, Thomas Hügle*

5. **Human cortical bone ECM proteome: the fingerprint of bone quality.** *Tatiana Kochetkova, Michael Stumpe, Jörn Dengjel, Jonathan Avaro, Bruno Silva, Antonia Neels, Andreas Borgschulte, Markus S. Hanke, Johann Michler, Philippe Zysset, Jakob Schwiedrzik*

6. **Effects of antidiabetic medications liraglutide, canagliflozin, and metformin on bone marrow adipose tissue in knee osteoarthritis: insights from an ex vivo model.** *Léa Loisay, Léonie Reinert, Alexander Antoniadis, Thibault Royon, Maja Kaegi, Elke Moradpour, Thomas Hügle, Jeroen Geurts*

7. **Cellular Uptake and Long-Term Retention of Gadolinium in Bone After Macrocyclic GBCA Exposure.** *N. Peyer, I. Jenni, R. Egli, B. Gantenbein, L. Goveas, J.T. Heverhagen, H. von Tengg-Kobligk, N. Ruprecht*

8. **Multi- vs. single-stack HR-pQCT scans of distal skeleton: impacts on geometry, micro architecture, and strength.** *Simone Poncioni, Alexia Pollaci, Kurt Lippuner, Philippe Zysset*

9. **In-vivo Quantification of Subchondral Bone Remodeling in osteoarthritic rat knees using the MIA model.** *Reitzel Antoine, Pioletti Dominique, Stadelmann A Vincent*

10. **EasyIPL: A High-Level Scripting Interface for SCANCO MicroCT Image Analysis.** *Vincent A. Stadelmann*

11. **Inhibition of PDGFRβ signaling in LepR^{+} osteoprogenitors by long-term sclerostin-neutralizing antibody treatment limits bone formation through progenitor pool exhaustion.** *Thouverey C, Gerbaix M, Badoud I, Apostolides P, Ferrari S.*

SBMS SUMMER SCHOOL ABSTRACTS

1. **An Injectable Type II Collagen/Hyaluronic Acid Hybrid Cell Carriers – A Step Towards an Extracellular Matrix-Inspired Scaffold for Regeneration Applications.** *Parisa Torabi Rahvar, Mohammad J. Abdekhodaie, Benjamin Gantenbein*

2. **The Cyto-Compatibility of Biomimetic Bombyx mori Silk and Growth and Differentiation Factor 5 (GDF5).** *Ashish Kumar, Sophie van Leemput, Sónia Filipa Fernandes Marques, Parisa Torabi Rahvar, Michael Wöltje, Benjamin Gantenbein*

SBMS 1

Shape Variability of the Medullary Canal of the Human Proximal Femur

Stefan Bracher[1], Benjamin Haas[2], Elhadi Sariali[3], Philippe Zysset[1]
[1]University of Bern, ARTORG Center for Biomedical Engineering Research, Bern, Switzerland, [2]Symbios Orthopédie SA, Yverdon-les-Bains, Switzerland, [3]Hôpital Pitié Salpêtrière, Paris, France.

Background: Proximal femoral morphology plays a critical role in the design and placement of cementless femoral stems in total hip arthroplasty (THA). Due to inter-patient variability influenced by genetics, lifestyle, and age-related changes, understanding medullary canal geometry is essential to optimize implant performance.

Objectives: This study aimed to characterize the geometric features of the human proximal femoral medullary canal and assess whether its shape can be captured using a limited set of morphological parameters.

Methods: Computed tomography (CT) scans of 763 individuals (389 females, 374 males; aged 20–92 years) were analyzed. Parameters extracted included medullary radius (R_{med}), medullary roundness index (MRI), cross-sectional orientation (φ), flare index (ratio of largest to smallest radius), and normalized curvature (L/R_{cur}). Variations were evaluated by sex and age. Additionally, a statistical shape model (SSM) was developed using principal component analysis (PCA).

Results: Geometric parameters showed clear sex- and age-specific trends, reflecting age-related bone remodeling. R_{med}/L increased more gradually proximally in older women (Fig. 1). MRI patterns were consistent across sexes, with minima near the gluteal tuberosity and lesser trochanter, and a maximum distal to the latter. Significant age-related differences in φ were observed only in females (p<0.01). The flare index was significantly higher in middle-aged and elderly males (p<0.001). L/R_{cur} showed sex- and age-dependency, especially in elderly males (p<0.01). The first three principal components of the SSM explained 68.4% of total shape variance and were each associated with at least one morphological parameter.

Conclusions: Proximal femoral medullary geometry varies significantly with sex and age. The derived parameters and shape models offer a framework for improved standard and personalized stem design, potentially reducing manual adjustments and material use in cementless THA.

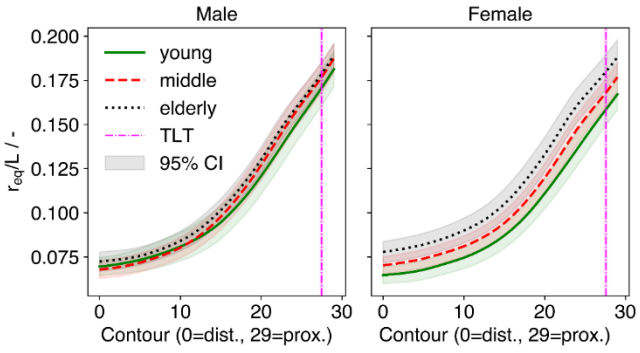

Fig. 1 Sex-, age-, and contour-specific mean Rmed/L with the location of the top of lesser trochanter (TLT) indicated.

SBMS 2

A novel bioreactor system to investigate the biomechanical characteristics of the supra spinatus entheses

Ćorluka Slavko[1,2], Spreng Joshua Dan[2], Gantenbein Benjamin[1,2], Schär Michael[1]

[1]IDepartment of Orthopaedic Surgery and Traumatology, Insel University Hospital, Faculty of Medicine, University of Bern, Switzerland [2]Tissue Engineering for Orthopaedics & Mechanobiology, Bone & Joint Program, Department for BioMedical Research (DBMR), Faculty of Medicine, University of Bern, Switzerland

Background: The shoulder balances mobility of the glenohumeral (GH) joint and stability of the rotator cuff (RC) muscles.[1] The extensive range of motion makes the shoulder prone to injuries. Entheses, 4-zoned tendon-to-bone attachment sites featuring (un-) mineralized fibrocartilage, are primarily affected by RC tears.[2] Existing models have not fully investigated the enthesis and thus are less applicable for translational orthopedics.

Objectives: 1.) Calibrate and validate a customized bioreactor to investigate the biomechanical response of shoulder entheses. 2.) Histologically analyze the influence of mechanical stimulation on entheses in sheep.

Methods: A customized bioreactor was calibrated and validated for applied forces, displacement, and frequency. Displacement validation was performed using video-based tracking with TrackMate for ImageJ 2.16.0. Sheep infraspinatus entheses (n=5 per condition) were subjected to sinusoidal uniaxial loading at either low (3%) or high (7%) strain for 1 hour daily. Control groups included day 0 samples and free-floating entheses (cultivated without mechanical loading). Samples were harvested at 7, 14, 21, and 28 days, sectioned, and stained with Alcian blue/orange G for semiquantitative analysis of the enthesis.

Results: The customized bioreactor demonstrated reliable performance with force measurements deviating by no more than 10.05% from true values (accuracy) with a reproducibility of ±2.53 N (precision). Maximum linear displacement measurements were accurate to within 3.21% of true values with a reproducibility of ±14.12%. Frequency control was maintained within 3.32% of target values with a reproducibility of ±3.72%. Alcian blue and Orange G staining revealed distinct four-zoned entheses with well-defined collagen fiber arrangements across all experimental conditions.

Conclusions: The bioreactor has sufficient precision and accuracy for research. Histology may reveal structural changes in entheses under different mechanical loading. Further research is needed to examine the effect of varying mechanical loading on entheses.

References

[1] Veeger, H.E.J. and F.C.T. Van Der Helm, *Shoulder function: The perfect compromise between mobility and stability.* Journal of Biomechanics, 2007. **40**(10): p. 2119-2129.
[2] Apostolakos, J., et al., *The enthesis: a review of the tendon-to-bone insertion.* Muscles, Ligaments and Tendons Journal, 2014. **4**(3): p. 333-342.

SBMS 3

What keeps cartilage attached to bone? New details at the osteochondral interface

Khizar Hayat[1], Aimee Colbath[2], Michael Doube[1]
[1]Department of Infectious Diseases and Public Health, Jockey Club College of Veterinary Medicine and Life Sciences, City University of Hong Kong, [2]Department of Clinical Sciences, College of Veterinary Medicine, Cornell University

Background: Strong attachment between articular calcified cartilage (ACC) and subchondral bone is vital to mammalian joint integrity, yet scant detail on the bonding between the two tissues exists.

Objectives: To determine the length scale at which bone and cartilage collagens interact, and to catalogue variations in osteochondral cement line formation.

Methods: Osteochondral samples were collected post-mortem from five sites in five horses and five cows, stored in 70% ethanol, then decalcified. Sections were cut and prepared for fluorescence and nanogold immunohistochemistry to localise type-I and type-II collagen, identifying subchondral bone and articular cartilage in confocal and transmission electron microscopies. Undecalcified

osteochondral blocks were trimmed to remove hyaline cartilage and all but a thin layer of subchondral bone. Osteoclasts were differentiated from bone marrow and seeded on orthogonal cut faces of the osteochondral blocks, and resorption pits measured with profilometry.

Results: Type-I and -II collagens form overlapping regions up to 5 µm deep containing hundreds of thousands to millions of colocalisation complexes per mm² of osteochondral cement line, at light microscopy resolution. TEM imaging placed type-I and -II collagens within a few tens of nm of each other. Osteoclastic resorption pits are deeper (2.5±0.18 vs 1.2±0.15 µm, $p < 0.001$) and rougher (2.4±0.17 vs 1.1±0.11 µm, $p = 0.041$) on ACC than bone, with the difference more pronounced in end-on pits than side-on pits. A bright band of type-II collagen immunoreactivity appeared in the osteochondral cement line in all bovine and no equine samples; osteochondral tears with both collagens on each side were present uniquely in bovine patella.

Conclusions: Bone and cartilage collagens interact at the osteochondral cement line, with notable variation among sites and between species. Osteoclastic resorption proceeds more rapidly on ACC than bone, leaving deeper and rougher pits depending on resorption direction relative to ACC collagen orientation.

SBMS 4

Uncovering Subchondral Bone and Marrow Cell-Specific Networks in Osteoarthritis through Integrative Correlation Analysis

Jeroen Geurts[1], Léa Loisay[1], Thomas Hügle[1]

[1]*Rheumatology, Lausanne University Hospital*

Background: Subchondral bone and its marrow adipose tissue undergo substantial remodeling during the progression of osteoarthritis. Characterizing cell type-specific transcriptional alterations is essential for elucidating the molecular mechanisms underlying disease pathogenesis and for the discovery of novel therapeutic targets. However, single-cell and spatial transcriptomic datasets required to enable such analyses are currently nonexistent.

Objectives: To decipher cell type-specific gene regulatory networks and signaling pathways within unfractionated osteoarthritis subchondral bone transcriptomes.

Methods: Differentially expressed genes were identified from three publicly available osteoarthritis transcriptomic datasets, comprising a total of 106 samples. DEGs were filtered based on cross-dataset overlap, the presence of proximal promoter transcriptional initiator elements, and known cell type-specific markers. A total of 359 upregulated and 268 downregulated genes were retained for integrative co-expression analysis aimed at resolving cell- and process-specific gene clusters. These clusters were subsequently subjected to bioinformatic analyses to infer gene regulatory networks (GRN) and signaling pathways.

Results: A total of 319 genes with an average correlation coefficient >0.65 were grouped into 9 distinct co-expression clusters (5 upregulated, 4 downregulated, *Figure below*). The downregulated clusters were enriched for gene signatures associated with adipocytes, vascular cells, and immune cells. These clusters were regulated predominantly by the transcription factors C/EBPα, SOX7, and SPI1/CREB5, respectively, and were linked to upstream signaling pathways including AMPK, insulin and Notch signaling. Upregulated clusters were enriched for osteocyte/osteoblast and pre-adipocyte signatures, regulated by the transcription factors Osterix, TWIST1, SNAI2 and PRRX1, and linked upstream to TGF-β and PDGF receptor signaling.

Conclusions: Integrative correlation analysis facilitated the deconvolution of subchondral bone and marrow adipose compartments, despite the current lack of comprehensive cell-specific transcriptomic atlases. Subsequent pathway and GRN analyses support therapeutic strategies aimed at enhancing AMPK signaling (e.g., via metformin) or inhibiting TGF-β and PDGF pathways in human knee osteoarthritis.

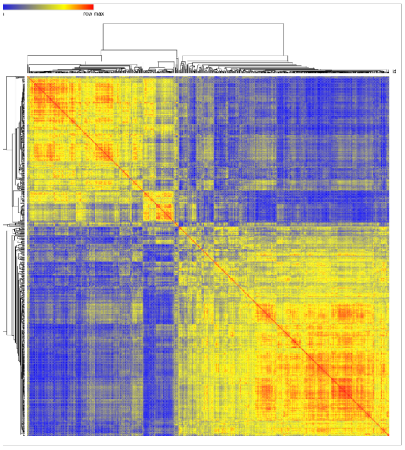

SBMS 5

Human cortical bone ECM proteome: the fingerprint of bone quality

Tatiana Kochetkova[1,2], Michael Stumpe[3], Jörn Dengjel[3], Jonathan Avaro[4], Bruno Silva[4], Antonia Neels[4], Andreas Borgschulte[5], Markus S. Hanke[6], Johann Michler[2], Philippe Zysset[1], Jakob Schwiedrzik[2,7]

[1]ARTORG Center for Biomedical Engineering Research, University of Bern, Switzerland, [2]Laboratory for Mechanics of Materials & Nanostructures, Empa - Swiss Federal Laboratories for Materials Science and Technology, Thun, Switzerland, [3]Metabolomics and Proteomics Platform, Department of Biology, University of Fribourg, Switzerland, [4]Center for X-ray Analytics, Empa - Swiss Federal Laboratories for Materials Science and Technology, St. Gallen, Switzerland, [5]Chemical Energy Carriers and Vehicle Systems Laboratory, Empa - Swiss Federal Laboratories for Materials Science and Technology, Dübendorf, Switzerland, [6]Department of Orthopedic Surgery, University Hospital of Bern, Switzerland, [7]Laboratory for High Performance Ceramics, Empa - Swiss Federal Laboratories for Materials Science and Technology, Dübendorf, Switzerland

Background: Emerging experimental evidence suggests that bone extracellular matrix (ECM)-level elastic and yield properties are remarkably constant in aging patients and remain unrelated to low-trauma fracture. However, it remains controversial whether the same is true for improved bone ECM composition, which may influence fracture initiation and propagation.

Objectives: Assessing cortical bone ECM composition in aging patients with and without the occurrence of femoral neck fracture to highlight potential compositional markers of bone quality.

Methods: Cortical bone samples of femoral neck inferomedial regions were collected during the total hip arthroplasty of 38 patients (45-89 y.o.) suffering from coxarthrosis (no fracture) or hip fracture, in accordance with the ethical approval 2018-01815 (Cantonal Ethics Commission of Bern, Switzerland). Liquid chromatography-mass spectrometry (LC-MS)-based proteomic analysis was complemented by Raman spectroscopy and FTIR to assess ECM chemical composition variations. On a subset of samples (N=18, 62-89 y.o.) SAXS/WAXS measurements were used to characterize the mineral fraction.

Results: From the complementary Raman spectroscopy and FTIR measurements, only mineral to matrix ratio showed a marginal increase in fracture patients ($p=0.04$), no significant differences in the ECM mineral characteristics from SAXS/WAXS were observed. Mineral platelet length and width were positively correlated with the mineral-to-matrix ratio ($p<0.004$). The overall ECM chemical composition and mineral morphology were constant with patient's age. Proteome analysis revealed a subtle distinction between patients with and without femoral neck fractures, specifically the overexpression of collagen trimers (e.g., COL16A1) in fracture patients. However, it is debatable whether these differences are consequences or causes of the fracture.

Conclusions: In contrast to spectroscopically derived compositional characteristics, ECM proteome measured via tandem LC-MS highlights potential markers of bone fragility. Despite the low number of patients, the proposed multimodal characterization approach yields new perspectives for organo-mineral bone matrix assessment.

SBMS 6

Effects of antidiabetic medications liraglutide, canagliflozin, and metformin on bone marrow adipose tissue in knee osteoarthritis: insights from an ex vivo model

Léa Loisay[1], Léonie Reinert[1], Alexander Antoniadis[2], Thibault Royon[2], Maja Kaegi[2], Elke Moradpour[1], Thomas Hügle[1], Jeroen Geurts[1]

[1] Rheumatology, Lausanne University Hospital [2] Orthopaedics, Lausanne University Hospital

Background: Bone marrow adipose tissue (BMAT) plays a key role in bone remodeling, especially under high energy demand conditions like osteoarthritis (OA). With rising OA risk factors like obesity and diabetes, targeting energy metabolism using anti-diabetic drugs like metformin, canagliflozin (SGLT2 inhibitor), and liraglutide (GLP1 receptor agonist) has gained interest as novel OA treatment. However, their effects on BMAT and bone remodeling remain unknown.

Objectives: This study investigates the effect of metformin, canagliflozin, and liraglutide on BMAT and bone metabolism in OA.

Methods: Non-sclerotic (NS) and sclerotic (SC) osteochondral tibial explant from OA patients (11) undergoing knee replacement were used. GLP1R and SGLT2 expression was assessed via IHC. Explants were treated for 7 days with each drug or vehicle. BMAT lipolysis (FFA, glycerol), bone formation (procollagen type I, ALP), and metabolic markers (IL-6, adiponectin) were analyzed.

Results: GLP1R and SGLT2 were expressed in BMAT (*Figure below*). All treatments significantly reduced FFA secretion in NS tissue (metformin: -31%; canagliflozin: -14.40%; liraglutide: -21.86%). Liraglutide and metformin reduced glycerol levels. In SC tissue, metformin had the strongest effects, significantly reducing FFA (-30%), glycerol and adiponectin. In SC samples, changes between treatment to vehicle revealed with canagliflozin a correlation between FFA and IL-6 ($r = 0.84$, $p = 0.001$), suggesting its role in regulating inflammation through lipolysis. Liraglutide showed a correlation between FFA and ALP ($r = 0.73$, $p = 0.009$), indicating an influence on bone activity. Metformin showed the strongest effects, with FFA and glycerol correlating with ALP ($r = 0.73$, $p = 0.01$) and procollagen type I ($r = 0.60$, $p = 0.04$), suggesting a direct impact on bone remodeling.

Conclusions: These findings reveal that anti-diabetic drugs can modulate BMAT lipolysis and may influence bone metabolism in OA. Long-term studies are needed to validate these effects and explore their therapeutic potential in OA management.

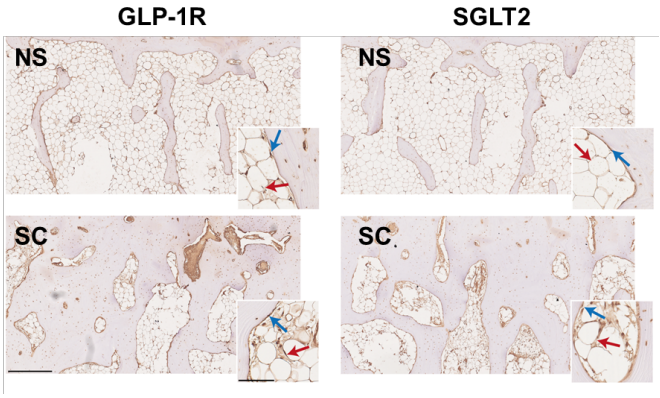

SBMS 7

Cellular Uptake and Long-Term Retention of Gadolinium in Bone After Macrocyclic GBCA Exposure

N. Peyer[1,2*], I. Jenni[1,2*], R. Egli[1], B. Gantenbein[2,3], L. Goveas[1,2], J.T. Heverhagen[1,2], H. von Tengg-Kobligk[1,2], N. Ruprecht[1,2]

[1]Department of Diagnostic, Interventional, and Pediatric Radiology, Inselspital, Bern University Hospital, University of Bern, Bern, Switzerland, [2]Department for BioMedical Research (DBMR), University of Bern, Bern, Switzerland, [3]Department of Orthopedic Surgery and Traumatology, Inselspital, Bern University Hospital, University of Bern, Bern, Switzerland

**presenting-authors*

Background: Gadolinium-based contrast agents (GBCAs) are widely used in MRI diagnostics. While macrocyclic agents are considered stable, gadolinium (Gd) retention in bone has been detected years after administration, raising concerns about potential long-term effects. The mechanisms underlying this long-term retention remain unclear.

Objectives: This study investigates the biodistribution and cellular uptake of GBCA in white blood cells (WBCs), bone marrow cells (BMCs), and bone compartments of mice, as well as lymphoblast cells (K562) and primary osteoblasts.

Methods: Eight-week-old mice received intravenous Gd-DOTA (1.2 mmol/kg bw). Gd content in WBCs and BMCs (1 hour and 28 days post-injection) was analyzed by single cell-inductively coupled plasma-mass spectrometry (SC-ICP-MS). Gd levels in bone epiphyses and diaphyses were assessed using ICP-MS. Similarly, Gd uptake was studied in osteoblasts and K562 cells under pre-determined concentrations using SC-ICP-MS.

Results: Gd was detected in both WBCs and BMCs at 1h post-injection, and only in BMCs at 28 days, indicating long-term retention. Higher Gd levels were observed in epiphyses than diaphyses, correlating with trabecular bone activity. Furthermore, osteoblasts showed Gd uptake, and K562 cells exhibited time-, concentration-, temperature- and energy-dependent uptake that followed Michaelis-Menten kinetics (v_{max} 1.18 x 10^{-11} [mol/g protein*s], K_m 1.3 mM).

Conclusions: Measurable gadolinium retention in bone marrow following exposure to macrocyclic GBCAs has been observed, suggesting that even the most stable agents may contribute to long-term Gd deposition. The uptake characteristics in lymphoblast are consistent with a carrier-mediated mechanism. These findings highlight the need to investigate the cellular and molecular pathways of GBCA retention and clearance, particularly in bone.

SBMS 8

Multi- vs. single-stack HR-pQCT scans of distal skeleton: impacts on geometry, micro architecture, and strength

Simone Poncioni[1,2], Alexia Pollaci[1], Kurt Lippuner[2], Philippe Zysset[1]

[1]ARTORG Center for Biomedical Engineering Research, University of Bern, Switzerland, [2]Department of Osteoporosis, University Hospital Bern, Switzerland

Background: Recent studies have reported reference data of bone microarchitecture in adults using second-generation HR-pQCT over ~10 mm sections. However, the thin section may miss weak regions where most fractures occur. To address this limitation, a multi-stack scanning protocol was developed to double and triple the section thickness at the distal radius and tibia.

Objectives: To compare and assess the relationships between multi- and single-stack HR-pQCT acquisition protocols.

Methods: Using a multi-stack protocol, Second-generation HR-pQCT images were acquired from healthy, young participants (22–37 y.o., 60M, 54F). Images were cropped to single-section equivalents. Image processing followed the standard workflow from the scanner's

manufacturer (IPL Scanco V5.16). Our latest hFE pipeline was used to estimate stiffness and yield force. Primary outcomes included densitometric parameters (Tt.vBMD, Ct.vBMD, Tb.BVTV), a size-independent geometrical parameter (Rel.Ct.Th), and mechanical parameters (stiffness S, yield force Fy). Relationships were evaluated through linear regression.

Results: All densitometric parameters showed strong correlations between multi- and single-stack images R2≥ 0.86. Geometrical parameters differed significantly at both sites (Fig 1, Rel.Ct.Th: yR=0.83x+0.02 R2=0.77, yT=0.58x+0.01 R2=0.93). Fy was underestimated by single-stack (Fig 2, yR=1.01x+2.99 R2=0.51, yT=0.93x+5.22 R2=0.73).

Conclusions: The findings show a strong correlation between densitometric parameters from multi- and single-stack protocols, supporting cross-study and cross-protocol comparisons. In contrast, size-independent geometrical parameters highlight the predominance of cortical thickness in single-stack sections, which thins distally. Multi-stack models exhibit lower stiffness and weaker correlations due to the increased size and shape difference. In contrast, Fy increases in multi-stack models, likely due to the higher capability of storing elastic energy prior to yielding due to the larger volume of the simulated body.

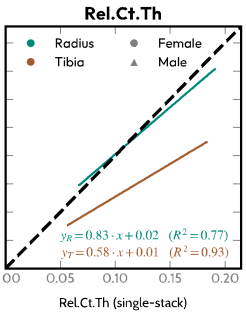

Fig 1: Relative cortical thickness: multi- vs. single-stack comparison

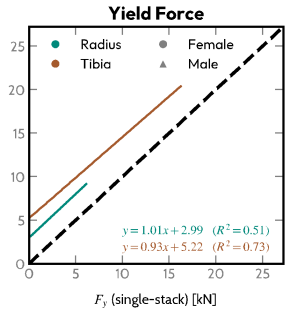

Fig 2: Yield force – multi- vs. single-stack comparison

SBMS 9

In-vivo Quantification of Subchondral Bone Remodeling in osteoarthritic rat knees using the MIA model.

Reitzel Antoine[1], Pioletti Dominique[1], Stadelmann A Vincent[2]
[1] *Biomechanical Orthopedics Laboratory – EPFL,* [2] *Schulthess Klinik*

Background: Osteoarthritis (OA) is a degenerative joint disease characterized, among others, by cartilage degradation and subchondral bone remodeling. While the monosodium iodoacetate (MIA) rat model is commonly used in OA research, standard dose applications often lead to rapid and severe joint destruction. Investigating the effects of low-dose MIA, a largely unexplored condition, may better represent the early and progressive stages of OA, making the model more suitable for therapeutic studies.

Objectives: To characterize subchondral bone remodeling over time in a low-dose MIA-induced OA model using *in vivo* micro-computed tomography (µCT).

Methods: Twenty rats were used, with the left knee injected with MIA and the right serving as a saline-injected control. Two MIA concentrations were tested: a standard dose (1 mg/50 µL) and a low dose (0.2 mg/50 µL). Cartilage degradation was assessed histologically, while longitudinal changes in subchondral bone were monitored using in vivo µCT. An automated image-processing pipeline was developed using *EasyIPL* that performs 3D image registration, bone segmentation, morphometric analysis, and 3D mapping of remodeling regions. This method reduces manual intervention and increases reproducibility across time points.

Results: The automated method successfully identified structural changes in subchondral bone over time. Distinct patterns were observed across groups: visible bone erosions with the standard MIA dose at the periphery of articular condyles, superficial changes with the low dose, and no effects in the control group (Fig 1). These results correlated with early cartilage damage seen in histology.

Conclusions: The developed µCT post-processing pipeline offers a fast and reliable solution for tracking bone remodeling in OA models. Its ability to detect changes at low MIA doses over the full bone surface supports its application in preclinical studies aiming to evaluate early OA progression and therapeutic interventions.

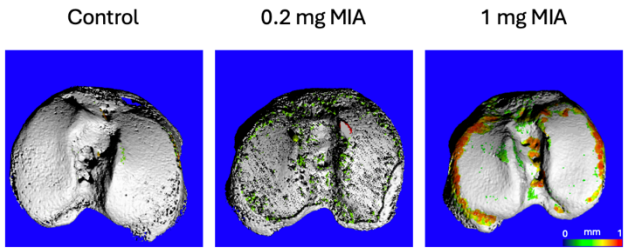

Figure 1. Comparison of subchondral resorption with 0, 0.2 and 1mg MIA.

SBMS 10

EasyIPL: A High-Level Scripting Interface for SCANCO MicroCT Image Analysis

Vincent A. Stadelmann[1,2]
[1]*Schulthess Klinik, Zürich,* [2]*Stadelmann Research Consulting, Switzerland*

Background: Despite the high image quality provided by SCANCO microCT systems, their software environment remains severely outdated. The core Image Processing Language (IPL), a terminal-based system on OpenVMS workstations, is cumbersome, verbose, and ill-suited for the evolving needs of modern musculoskeletal research. Standard workflows in IPL require long linear scripts with complex multi-line functions and lack direct access to image properties for dynamic parameterization. Moreover, scripting often necessitates switching between IPL and the Digital Command Language (DCL) to perform basic tasks such as reading metadata from log files—a process both error-prone and inefficient.

Methods: To address these limitations, we developed EasyIPL (www.easyipl.com), an open-source high-level macro library that wraps SCANCO IPL and DCL into a unified, object-oriented-like scripting interface. EasyIPL integrates direct access to image properties, eliminating the need to exit IPL for metadata retrieval. It simplifies common multi-step processing pipelines into single-line macros, reducing script length by up to 80%. Additionally, it offers built-in support for vector operations and 3D spatial transformations, further enhancing automation and reproducibility.

Results: EasyIPL has been successfully applied in numerous studies, including those on implant integration and infection[1], bone adhesives[2], osteoarthritis[3], atherosclerosis[4] and vertebroplasty[5]. It has been adopted by several students with minimal prior coding experience for image analysis, all of whom reached scripting proficiency within weeks—contrasting with the typical 1+ year learning curve for native IPL.

Conclusions: By bridging legacy systems with modern research demands, EasyIPL enables more flexible, efficient, and scalable microCT analysis workflows, supporting the growing complexity and customization required in contemporary musculoskeletal imaging research.

References:

[1] V. A. Stadelmann, K. Thompson, S. Zeiter, K. Camenisch, U. Styger, S. Patrick, A. McDowell, D. Nehrbass, R. G. Richards, T. F. Moriarty, *Sci Rep* **2020**, *10*, 20901.
[2] A. J. Bojan, V. A. Stadelmann, D. Wu, M. Pujari-Palmer, G. Insley, D. Sundh, C. Persson, H. Engqvist, P. Procter, *Injury* **2022**, *53*, 1858.
[3] M. Keiser, S. Preiss, S. J. Ferguson, V. A. Stadelmann, *Bone* **2025**, *193*, 117388.
[4] V. A. Stadelmann, G. Boyd, M. Guillot, J. Bienvenu, C. Glaus, A. Varela, *International Journal of Biomedical Imaging* **2021**, *2021*, 1.
[5] V. A. Stadelmann, I. Zderic, A. Baur, C. Unholz, U. Eberli, B. Gueorguiev, *Medical Engineering & Physics* **2016**, *38*, 97.

SBMS 11

Inhibition of PDGFRβ signaling in LepR$^+$ osteoprogenitors by long-term sclerostin-neutralizing antibody treatment limits bone formation through progenitor pool exhaustion

Thouverey C, Gerbaix M, Badoud I, Apostolides P, Ferrari S.
Service of Bone Diseases, University Hospital of Geneva, Geneva, Switzerland

Background: The transient bone anabolic effects of anti-sclerostin antibody (Scl-Ab) may be partially explained by the depletion of osteoprogenitors (OPs) capable of differentiating into bone-forming osteoblasts.

Objectives: Since PDGFRβ signaling promotes OP self-renewal and recruitment while inhibiting their differentiation into osteoblasts, we investigated the role of PDGFRβ in leptin receptor-positive (LepR$^+$) OPs in response to Scl-Ab treatment.

Methods: Four-month-old *Lepr-Cre* (control) and *Lepr-Cre;Pdgfrbf/f* (PDGFRβ-deficient in LepR$^+$ OPs) mice received subcutaneous injections of 50 mg/kg of Scl-Ab or vehicle for 2 or 6 weeks. To evaluate whether a treatment-free interval could restore bone formation following prolonged Scl-Ab exposure, both genotypes also underwent intermittent Scl-Ab treatment (2 weeks of Scl-Ab, followed by 2 weeks of vehicle, then 2 additional weeks of Scl-Ab).

Results: *Lepr-Cre* and *Lepr-Cre;Pdgfrbf/f* mice exhibited similar baseline bone phenotypes. PDGFRβ deletion in LepR$^+$ cells enhanced the short-term anabolic response to Scl-Ab (after 2 weeks: +24.5% trabecular BV/TV, p=0.005; +25.5% trabecular BFR, p=0.016; +37.9% serum PINP, p=0.043) but did not prevent its attenuation after prolonged treatment (6 weeks), with trabecular BFR and osteoblast numbers returning to baseline in both genotypes. The reduction in bone formation correlated with a decreased number of LepR$^+$ OPs at 2 and 4 weeks (-42% and -65%, p=0.0001), more pronounced in *Lepr-Cre;Pdgfrbf/f* mice. In control mice, both LepR$^+$ OP numbers and the anabolic response to Scl-Ab were restored following a 2-week treatment-free period (+66.3% trabecular BFR, p=0.0004; +60.8% osteoblast number per bone perimeter, p=0.0001), an effect not observed in PDGFRβ-deficient mice. Finally, in the KUSA-A1 OP cell line, Scl-Ab inhibited sclerostin-induced co-activation of PDGFRβ signaling and expression of proliferation regulators c-Myc and c-Jun.

Conclusions: PDGFRβ signaling in LepR$^+$ cells is essential for maintaining a sufficient pool of Wnt-responsive OPs during Scl-Ab treatment, thereby supporting sustained bone formation.

SBMS SUMMER SCHOOL 1

An Injectable Type II Collagen/Hyaluronic Acid Hybrid Cell Carriers – A Step Towards an Extracellular Matrix-Inspired Scaffold for Regeneration Applications

Parisa Torabi Rahvar[1], Mohammad J. Abdekhodaie[2,3], Benjamin Gantenbein[1,4]

[1]Tissue Engineering for Orthopaedics & Mechanobiology, Bone and Joint Program, Department for BioMedical Research (DBMR) of the Medical Faculty, University of Bern, Bern, Switzerland.
[2]Department of Chemical Engineering, Sharif University of Technology, Tehran, Iran
[3]Environmental and Applied Science Management, Yeates School of Graduate Studies, Toronto Metropolitan University, Toronto, Canada
[4]Department of Orthopaedic Surgery and Traumatology, Inselspital, Bern University Hospital, Medical Faculty, University of Bern, Bern, Switzerland

Background: The extracellular matrix (ECM) plays a vital role in regulating cellular functionality and tissue regeneration, providing both compositional and architectural cues [1]. In this study, type II collagen (COL-II) and hyaluronic acid (HA), as the main components of cartilage tissues like articular nucleus pulposus and cartilage, were used to design an injectable bioinspired hydrogel scaffold for tissue regeneration.

Objectives: This work presents a method for creating hydrogels and microgels from HA and COL-II to encapsulate and deliver mesenchymal stem cells (MSCs). The characterization of these carriers is performed to evaluate their potential in enhancing cartilage tissue regeneration.

Methods: COL-II and HA were chemically modified and crosslinked to encapsulate MSCs. We characterized the chemical, physical, and mechanical properties of hydrogels, as well as the effects of composition on MSC viability and function [1]. Microgels were also prepared using a flicking-based method with HA/COL-II composition [2].

Results: Increasing the HA content led to higher storage modulus and reduced hydrogel shrinkage. Encapsulated MSCs survived well in all the hydrogels. Incorporating COL-II into HA-Tyr hydrogels created a more favorable microenvironment for chondrogenic differentiation. Compared to HA alone, the hybrid HA-Tyr/COL-II hydrogel promoted enhanced cell adhesion, spreading, proliferation, and upregulation of cartilage-related gene expression.

Conclusions: The injectable HA-Tyr/COL-II hybrid hydrogels benefit from the enhanced mechanical strength of HA and cell adhesive, proliferative, and chondrogenic conductive properties of COL-II. These results highlight the promising potential of this hybrid system as a biomaterial scaffold for nucleus pulposus or cartilage regeneration applications, delivering cells in a supportive and bioactive microenvironment.

Acknowledgments: This Research was financed by a Weave Agency Grant of the Swiss National Science Foundation (# 320030E_224175) and the German Research Society (Deutsche Forschungsgemeinschaft, DFG, # 437213841).

References:

[1]. Torabi P. et al., Int. J. Biol. Macromol. 279 (2024): 134614.
[2]. Torabi P. et al., J Drug Deliv Sci Technol (2025): 106921.

SBMS SUMMER SCHOOL 2

The Cyto-Compatibility of Biomimetic Bombyx mori Silk and Growth and Differentiation Factor 5 (GDF5)

Ashish Kumar[1,2], Sophie van Leemput[1], Sónia Filipa Fernandes Marques[1], Parisa Torabi Rahvar[1,4], Michael Wöltje[3], Benjamin Gantenbein[1,4]

[1] *Tissue Engineering for Orthopaedics & Mechanobiology, Bone and Joint Program, Department for BioMedical Research (DBMR) of the Medical Faculty, University of Bern, Bern*
[2] *Graduate School for Cellular and Biomedical Sciences (GCB), University of Bern*
[3]*Institute of Textile Machinery and High-Performance Material Technology, TUD University of Technology, Dresden, Germany*
[4]*Department of Orthopaedic Surgery and Traumatology, Inselspital, Bern University Hospital, Medical Faculty, University of Bern, Bern*

Background: Low back pain (LBP) is a major global burden of disability, often caused by degeneration ofthe intervertebral disc (IVD). Current treatments focus on symptom management and fail to offer long-term regenerative solutions. Silk fibroin has emerged as a promising biomaterial for orthopaedics in general, also for IVD repair due to its excellent biocompatibility and tunable mechanical properties.

Objectives: This study investigated the potential of fiber-based additive-manufactured (FAM) silk scaffolds compared to a silk fiber fleece composite using a silk extrusion 3D printing technology (Frauchiger et al.), produced by Spintec Engineering, Aachen, Germany). Additionally, the effect of GDF5 was evaluated.

Methods: Human bone-marrow-derived mesenchymal stromal cells (hMSCs) collected from vertebrae during spinal surgery were expanded up to P2-P3 in α-modified Eagle Medium (MEM). 600k cells were seeded on each silk scaffold (5×5 mm for fleece; 5 mm diameter × 3 mm height for FAM) and cultured in low-glucose Dulbecco's Modified Eagle Medium (LGDMEM) and were allowed to settle for 24h. For 3D culture, the medium was replaced with chondrogenic inductive medium and 100 ng/mL GDF5. DNA and GAG quantification were done. Cytocompatibility was assessed using Live/Dead staining. Confocal laser scanning microscopy (cLSM) was performed using z-stacks and tile scans of the scaffolds.

Results: Live/Dead staining showed >90% of viable cells on both scaffolds at day 7, but <20% of cells were viable at day 14. GDF5 significantly enhanced cell viability and attachment on both silk fleece and FAM silk scaffolds on day 7. The GAG quantification showed that FAM-silk with GDF5 exhibited the highest GAG content and was increased by day 14, outperforming 3D printed silk without GDF5. The DNA quantification showed that the 3D-printed silk with showed the highest DNA and GAG levels by day 14, indicating superior cell proliferation and matrix synthesis. In contrast, FAM-silk with GDF5 supported proliferation but low GAG production, while 3D-printed silk without GDF5 showed minimal cell growth, highlighting the scaffold-dependent effect of GDF5 (n=1).

Conclusions: 3D-printed silk with GDF5 supports superior cell viability, proliferation, and GAG production over 14 days. GDF5 improves early cell attachment on both scaffolds, but only 3D printed silk maintains function long-term. FAM silk fails to support sustained matrix production.

Acknowledgments: This Research was financed by a Weave Agency Grant of the SwissvNational Science Foundation (# 320030E_224175) and the German Research Society (Deutsche Forschungsgemeinschaft, DFG, # 437213841). We thank Yamina Baumgartner for assistance with assays.